RAPID COMMUNICATIONS

PHYSICAL REVIEW A VOLUME 47, NUMBER 4 APRIL 1993

Hyperfine quenching and measurement of the $2\,^3P_0-2\,^3P_1$ fine-structure splitting in heliumlike silver (Ag^{45+})

Bruce B. Birkett
Department of Physics, University of California, Berkeley, California 94720

Jean-Pierre Briand and Pierre Charles
Laboratoire de Physique Atomique et Nucléaire (LPAN), Institut de Radium, Université Pierre et Marie Curie, T12, Boîte 93, 75252 Paris, CEDEX 05, France

Daniel D. Dietrich
Lawrence Livermore National Laboratory, L-296, P.O. Box 808, Livermore, California 94550

Keith Finlayson
Gesellschaft für Schwerionenforschung m.b.H., 6100 Darmstadt, Germany

Paul Indelicato
Laboratoire de Physique Atomique et Nucléaire (LPAN), Institut de Radium, Université Pierre et Marie Curie, T12, Boîte 93, 75252 Paris, CEDEX 05, France

Dieter Liesen
Gesellschaft für Schwerionenforschung m.b.H., 6100 Darmstadt, Germany

Richard Marrus
Department of Physics, University of California, Berkeley, California 94720

Alexandre Simionovici
Laboratoire Grenoblois de Recherches sur les Ions, les Plasmas et la Physique Atomique (LAGRIPPA), Centre d'Etudes Nucléaires de Grenoble, B.P. 85X, 38041 Grenoble CEDEX, France

(Received 28 September 1992)

The hyperfine-quenched transition $2\,^3P_0$–$1\,^1S_0$ has been observed in heliumlike silver (Ag^{45+}) in the two isotopes ^{107}Ag and ^{109}Ag. The lifetime for the transition has been measured for each isotope and found to be $\tau_0(107)=3.98(37)\times10^{-12}$ sec and $\tau_0(109)=2.84(32)\times10^{-12}$ sec. From the measured lifetimes a value is inferred for the absolute value of the $2\,^3P_0$–$2\,^3P_1$ fine-structure splitting $|\Delta E_{0-1}|$ in Ag^{45+} with the result $|\Delta E_{0-1}|=0.79(04)$ eV, where the uncertainty is the experimental uncertainty taken at the 1σ confidence level. This result is compared with calculations based on the multiconfigurational Dirac-Fock method, the unified method, and recent results from the relativistic configuration-interaction method.

PACS number(s): 32.30.Rj, 12.20.Fv, 31.30.Jv, 32.70.Fw

The fine-structure splittings of the $(1s)(2p_{1/2})\,2\,^3P_J$ states [1] in two-electron ions ($\Delta E_{J\text{-}J'}$) are determined largely by the electron-electron interaction. The measurement of these splittings constitutes, therefore, a test of theories of this interaction in the simplest atomic system in which it can be observed. Because of the rapid scaling of the relativistic part of this interaction with atomic number Z, measurements at high Z provide a particularly sensitive test of the relativistic theory. Calculations of fine-structure splittings generally include the effects of relativity by a perturbation expansion in the parameter $(Z\alpha)^2$. The problems associated with this approach at high Z are illustrated by the fact that in ordinary helium ($Z=2$) the calculations are accurate at the ppm level, whereas the most elaborate calculations at $Z=47$ are accurate at only the few percent level [2,3].

The measurement reported here is of the interval ΔE_{0-1} in the two-electron ion Ag^{45+}. In even-even isotopes with nuclear spin $I=0$, the radiative decay $2\,^3P_0$–$1\,^1S_0$ is strictly forbidden and the $2\,^3P_0$ state undergoes an $E1$ decay to the $2\,^3S_1$ state with a calculated lifetime [4] of $\tau(2\,^3P_0)=8.598\times10^{-10}$ sec. Silver has, however, two stable isotopes with nuclear spin $I=\frac{1}{2}$, ^{107}Ag and ^{109}Ag, which have nuclear magnetic moments $\mu(^{107}Ag)=-0.1135\mu_N$ and $\mu(^{109}Ag)=-0.1305\mu_N$ [5]. These isotopes exhibit hyperfine coupling which causes a mixing of the $2\,^3P_0$ and $2\,^3P_1$ states. The $2\,^3P_1$ state decays rapidly by an $E1$ transition to the $1\,^1S_0$ ground state with an unperturbed lifetime [4] of $\tau(2\,^3P_1)=6.211\times10^{-16}$ sec. The mixing induced by the hyperfine coupling therefore causes the perturbed $2\,^3P_0$ state to decay directly to the $1\,^1S_0$ ground state. A transition induced in this way is referred to as a hyperfine-quenched transi-

 ©1993 The American Physical Society

tion. These transitions are extremely rare in atomic physics, and were recently examined in Ni^{26+} [6].

Since the $2\,^3P_0$ and $2\,^3P_1$ states are very nearly degenerate in Ag^{45+}, the perturbed lifetime of the $2\,^3P_0$ state when hyperfine structure is present can be obtained with high accuracy by solving the two-level system:

$$\begin{vmatrix} E_0+i\frac{\Gamma_0}{2}-\lambda & W_{10} \\ W_{10} & E_1+W_{11}+i\frac{\Gamma_1}{2}-\lambda \end{vmatrix}=0\ , \qquad (1)$$

where $W_{10}=\langle 2\,^3P_0|H_{\rm hfs}|2\,^3P_1\rangle$, $W_{11}=\langle 2\,^3P_1|H_{\rm hfs}|2\,^3P_1\rangle$, and E_0,Γ_0 (E_1,Γ_1) are the unperturbed energies and radiative widths of the $2\,^3P_0$ $(2\,^3P_1)$ levels, respectively, and $H_{\rm hfs}$ is the hyperfine-structure Hamiltonian. The real and imaginary parts of λ_0 (λ_1) provide the perturbed energies and lifetimes of the $2\,^3P_0$ $(2\,^3P_1)$ levels. A fully relativistic calculation of the matrix elements has been made and the parameters Γ_0 and Γ_1 evaluated [4]. Values of these parameters for Ag^{45+} are given in Table I. Using these results with Eq. (1), a value of $|\Delta E_{0-1}|$ can be determined from the measured $2\,^3P_0$ lifetimes. This method was recently applied to Gd^{62+} [7], and has also been previously applied to $^{107}Ag^{45+}$ [8]. The precision of the $^{107}Ag^{45+}$ experiment was limited, however, by fluctuations in the beam position as well as the use of a single isotope. The measurement reported here reflects an improvement in precision by a factor of roughly 5.

This experiment was performed using the beam-foil time-of-flight technique on a 35-MeV/A silver beam provided by the GANIL accelerator (Caen, France). The extracted beam from the accelerator was passed through a 4.81-mg/cm^2 Be stripping foil, and emerged containing approximately 25% hydrogenlike silver (Ag^{46+}). The Ag^{46+} beam was separated from the other charge states by a high-resolution magnetic spectrometer system (LISE). The pure Ag^{46+} beam was then passed through a 400-μg/cm^2 carbon capture foil which produced the excited $2\,^3P_0$ state of Ag^{45+} of interest. The $2\,^3P_0$–$1\,^1S_0$ hyperfine-quenched transition from this state was then observed downstream of the foil by two solid-state detectors mounted on opposite sides of the beam, as shown in Fig. 1. One of the detectors was fixed and used for normalization purposes. The second detector was movable and the time-of-flight data were obtained by finding the ratio of counts in the movable detector to counts in the fixed detector as a function of the position of the movable detector. With this arrangement normalization is done directly to the ion population in the excited state of interest.

The initial beam energies prior to stripping were determined using the precise GANIL alpha spectrometer and were found to be $E_0(107)=36.4436$ MeV/A and $E_0(109)=35.0146$ MeV/A. The energy loss through the Be foil was measured using the GANIL LISE spectrometer, and was found to be in good agreement with published tables [9]. A correction was then made for the energy loss through the C foil based on published tables [9]. The final corrected velocities were found to be $\beta(107)=0.2675(1)$ and $\beta(109)=0.2622(1)$.

TABLE I. Parameter values (in eV) for Eq. (1).

A	W_{10}	W_{11}	Γ_0	Γ_1
107	−0.012 22	−0.015 31	7.656×10^{-7}	1.060
109	−0.014 05	−0.017 60	7.656×10^{-7}	1.060

A sample spectrum obtained with the movable detector is shown in Fig. 2. The large peak (22.6 keV) contains counts from the decay of interest $2\,^3P_0\rightarrow 1\,^1S_0$ as well as counts from the transition $2\,^3S_1\rightarrow 1\,^1S_0$. The second peak (22.8 keV) contains counts from the cascade decays $2\,^3P_2\rightarrow 1\,^1S_0$ and $2\,^1P_1\rightarrow 1\,^1S_0$. The third peak (23.2 keV) is due to transitions in the H-like (Ag^{46+}) ions that are excited in the carbon foil. Each spectrum from the movable and fixed detectors was fit by first subtracting a linear background determined by interpolating between the background counts on the low-energy and high-energy sides of the peaks. The peaks themselves were then fit to three Gaussians as shown in Fig. 2.

The raw data used to determine the lifetimes and the fine structure consist of similar spectra taken at many fixed-detector–movable-detector separations for each of the two isotopes $^{107}Ag^{45+}$ and $^{109}Ag^{45+}$. The curves obtained by taking the ratios of movable to fixed detector counts in the large peak (22.6 keV) at each detector position are shown in Figs. 3 and 4 for the two isotopes $^{107}Ag^{45+}$ and $^{109}Ag^{45+}$. Each decay curve was fit to the sum of two exponentials, corresponding to the transitions $2\,^3P_0\rightarrow 1\,^1S_0$ and $2\,^3S_1\rightarrow 1\,^1S_0$. A three-exponential combined fit to the two isotopes together was also performed. One exponential corresponded to the $2\,^3S_1\rightarrow 1\,^1S_0$ decay in both isotopes, since this decay length is independent of isotope once appropriate correction has been made for the differing velocities. One exponential was then used to fit the $2\,^3P_0\rightarrow 1\,^1S_0$ decay in each of the two isotopes. This combined fit yielded nearly identical results to the individual fits, and the results of the two types of fit were averaged to obtain the final measured decay lengths.

After correcting the measured decay lengths by the appropriate Lorentz contraction factors, the lifetimes of the $2\,^3S_1$ and $2\,^3P_0$ states were determined and are shown in Table II. No correction has been made for possible cas-

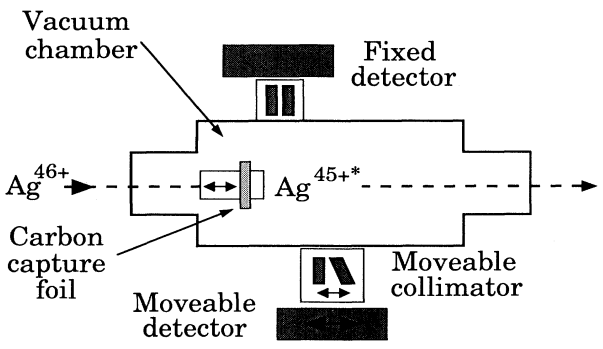

FIG. 1. Schematic design of the time-of-flight apparatus.

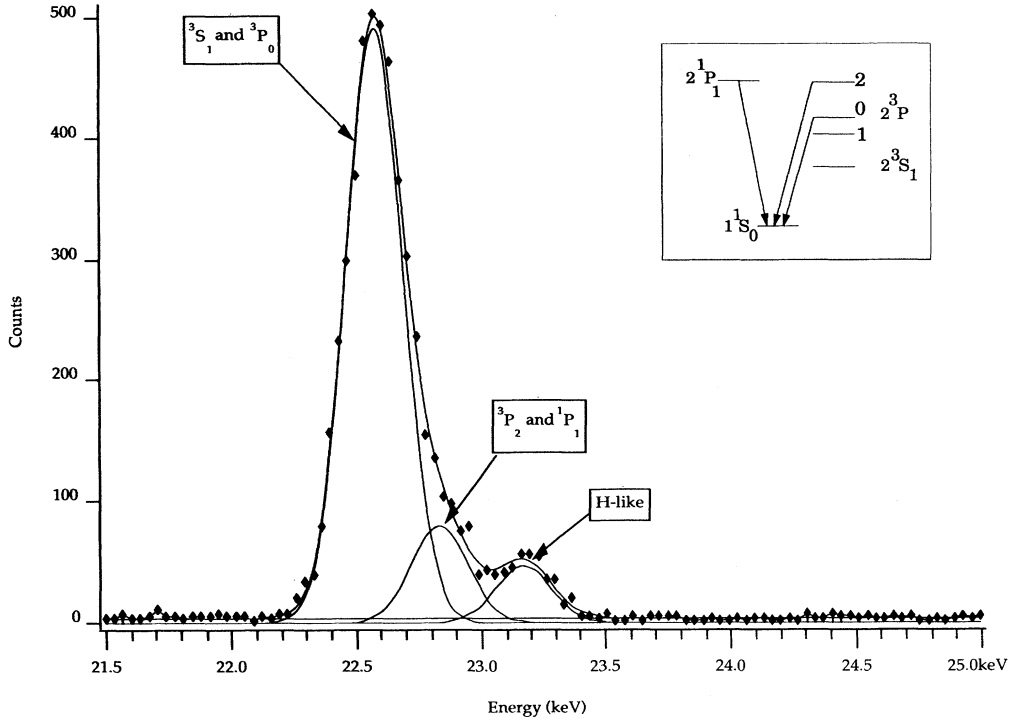

FIG. 2. Sample spectrum obtained by the movable detector 350 μm from the foil.

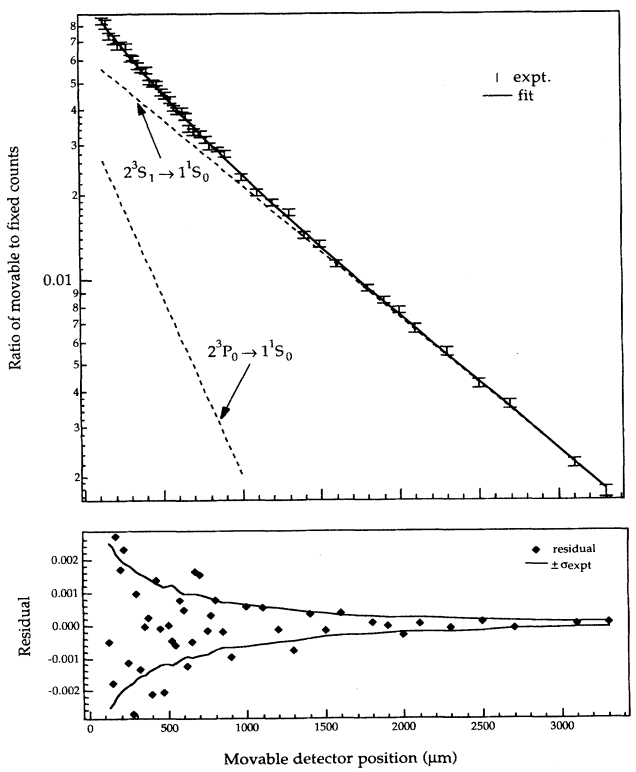

FIG. 3. Two-exponential fit to the radiative decay of the $2\,^3S_1$ and $2\,^3P_0$ states and fit residual for the isotope $^{107}Ag^{45+}$.

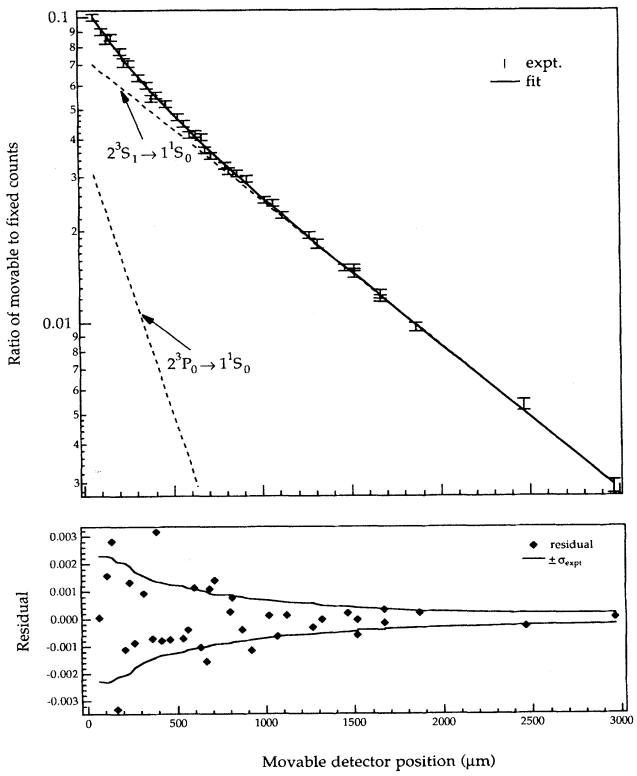

FIG. 4. Two-exponential fit to the radiative decay of the $2\,^3S_1$ and $2\,^3P_0$ states and fit residual for the isotope $^{109}Ag^{45+}$.

TABLE II. Lifetimes for the $2\,^3S_1$ and $2\,^3P_0$ states (values in sec).

A	$\tau(2\,^3S_1)$	$\tau(2\,^3P_0)$
107	$1.11(02)\times10^{-11}$	$3.97(37)\times10^{-12}$
109	$1.12(02)\times10^{-11}$	$2.84(32)\times10^{-12}$

cade contributions, but the residual plots shown in Figs. 3 and 4 show no monotonic residuals from the exponential fits. From the measured $2\,^3P_0$ lifetimes it is possible to deduce values for $|\Delta E_{0-1}|=|E_1-E_0|$ by using Eq. (1). We obtain $|\Delta E_{0-1}(107)|=0.81(05)$ eV and $|\Delta E_{0-1}(109)|=0.77(07)$ eV. The agreement between the two values of $|\Delta E_{0-1}|$ for the two different isotopes within the experimental error is an important check on the consistency of the experiment and the theoretical interpretation of the data. Taking a weighted average of $|\Delta E_{0-1}|$ for the two isotopes yields our final value $|\Delta E_{0-1}|=0.79(04)$ eV. We note that this uncertainty is less than 5% of the natural linewidth of roughly 1 eV for this transition.

The experimental errors are determined by uncertainties associated with the fitting procedures and are taken at the 1σ confidence level. Systematic error associated with the experiment arises mainly from uncertainty in the beam velocity, which is negligible. The error associated with the theory used to determine the fine-structure splitting from the measured lifetimes arises mainly from the estimated accuracy of Γ_1. Two of the other theoretical parameters, Γ_0 and W_{11}, have very little influence on the final result, and W_{10} is calculable to a high precision. The value of Γ_1 is determined from the MCDF code of Desclaux [3,4], and values using this method are in agreement with the variational calculations of Drake [10] and relativistic random-phase approximation calculations of Johnson and Lin [11] at the few percent level. Taking this level of agreement between the values obtained by the various methods as a measure of the uncertainty in theoretical parameters leads to an uncertainty of about 1% in the final reported value. We emphasize, however, that the final uncertainty stated with the reported $|\Delta E_{0-1}|$ value is the experimental uncertainty only and contains no allowance for possible theoretical error.

TABLE III. Experimental results and comparison with theory (values in eV).

	Experiment (This work)	MCDF method (Ref. [3])	Unified method (Ref. [2])	Relativistic CI (Ref. [13])
$\lvert\Delta E_{0-1}\rvert$	0.79(04)	0.753	0.933	0.788

The experimental value may be compared to three theoretical approaches as shown in Table III. The multiconfigurational Dirac-Fock (MCDF) method [3,12] has the effects of relativity built into the calculation from the beginning. Drake's unified method [2] begins with high-precision variational wave functions and energies, which are then used to treat the effects of relativity and quantum electrodynamics by perturbation theory. Our result is in agreement with the MCDF result, and differs by 3.5σ from the unified method value. Chen, Cheng, and Johnson have very recently completed relativistic configuration-interaction (CI) calculations [13]. These calculations begin with the construction of two-electron basis functions from configuration products of one-electron basis orbitals. The variational principle is then applied to determine the wave functions and energies of the states. The results include the Coulomb interaction and the retarded Breit interaction, and are corrected for QED and mass polarization effects using Drake's unified method results. This relativistic CI result is in excellent agreement with the reported experimental value.

This work was supported by NSF Grant No. PHY9100505, by NATO Grant No. CRG900630, by LLNL Contract No. W-7450-ENG-48, and by the Centre National de la Recherche Scientifique, France. LPAN is Unité Associé au CNRS No. 771, and LAGRIPPA is Unité Mixte de Recherche du CNRS No. 038. The authors would like to thank the GANIL staff for their complete and excellent support during this experiment.

[1] In this paper we use as a matter of convenience the L-S coupling notation $2\,^3P_1$ to denote the state $(1s_{1/2})(2p_{1/2})J=1$. Strictly speaking, the actual state in Ag^{45+} is much closer to the j-j coupling limit than it is to the L-S coupling limit.

[2] G. W. F. Drake, Can. J. Phys. **66**, 586 (1988).

[3] O. Gorceix, P. Indelicato, and J. P. Desclaux, J. Phys. B **20**, 639 (1987).

[4] P. Indelicato, F. Parente, and R. Marrus, Phys. Rev. A **40**, 3505 (1989).

[5] G. H. Fuller, J. Phys. Chem. Ref. Data **5**, 835 (1976).

[6] R. W. Dunford, C. J. Liu, J. Last, N. Berrah-Mansour, R. Vondrasek, D. A. Church, and L. J. Curtis, Phys. Rev. A **44**, 764 (1991).

[7] P. Indelicato, B. B. Birkett, J. P. Briand, P. Charles, D. D. Dietrich, R. Marrus, and A. Simionovici, Phys. Rev. Lett. **68**, 1307 (1992).

[8] R. Marrus, A. Simionovici, P. Indelicato, D. D. Dietrich, P. Charles, J. P. Briand, K. Finlayson, F. Bosch, D. Liesen, and F. Parente, Phys. Rev. Lett. **63**, 502 (1989).

[9] F. Hubert, R. Bimbot, and H. Gauvin, At. Data Nucl. Data Tables **46**, 1 (1990).

[10] G. W. F. Drake, Phys. Rev. A **19**, 1387 (1979).

[11] W. R. Johnson and C. D. Lin, Phys. Rev. A **14**, 565 (1976).

[12] J. Hata, J. Phys. B **17**, L241 (1984); J. Hata and I. P. Grant, *ibid.* **16**, 523 (1983); **17**, 931 (1984); W. R. Johnson and C. D. Lin, Phys. Rev. A **14**, 565 (1976); C. D. Lin, W. R. Johnson, and A. Dalgarno, *ibid.* **15**, 154 (1977).

[13] M. H. Chen, K. T. Cheng, and W. R. Johnson, (to be published).